2-PASS DIFFERENTIAL INTERFEROMETRY IN THE AREA OF THE SLATINICE ABOVE-LEVEL DUMP

Milan BOŘÍK[1]

[1]Department of Mathematics, Faculty of Civil Engineering, Czech Technical University in Prague, Thákurova 7, 166 29, Prague,
borikm@mat.fsv.cvut.cz

Abstract

We concentrate on areas with abandoned open brown coal mines, or undermined areas. We made analyzes of terrain deformation in the area of the Slatinice above-level dump that is monitored because of potential terrain deformations. The 2-pass differential interferometry method was used. Interferometric processing was performed in the GAMMA software. The differential interferogram for the 2-pass method was filtered and then unwrapped. Due to filtering we achieved much better coherence. Unwrapped phase of that differential interferogram can be used for a terrain-deformation detection more profitably. An important feature of this method is that all measurements are relative. Theoretically, the phase of the differential interferogram should be zero in the areas of no deformation, but there are systematic errors influencing the measurements and therefore the deformations can be determined only relatively with respect to the vicinity. Expected deformations can be described quantitatively. For decision on potential terrain deformation, the suspect areas of subsidence must be sufficiently coherent. For incoherent areas there occurs decorrelation and thus loss of data. For subsidence confirmation, we demand as continuous phase as possible with a sufficient number of neighboring pixels and lines. Further we concentrated on the Jirkov-Most route and railway that slides and is also monitoring and leveled very precisely. Especially its part called the Ervenice corridor. We cannot evidence that area of the Ervenice corridor is stable because of larger variance of the unwrapped-phase values. The results are very decorrelated. In this area, we verified no terrain deformation.

Keywords: differential interferometry, 2-pass method, undermined areas, dumps

INTERFEROMETRY

Interferometry is method [1], that use coherent radiation to determine space relations on the Earth surface. Satellites with synthetic aperture radar (SAR) scan the same area under little different visual angle. SAR was developed due to bad radar resolution with the real aperture. By means of Doppler effect of frequency modulation, SAR substitutes the length of antennas by modified measurement art. Two satellites (ERS-1, ERS-2) flies the same orbits in a given time interval. Distance between both satellites is called interferometric baseline and its perpendicular projection into the slant range is called perpendicular baseline. Radar apertures get data containing intensity (that describes reflex possibility of the surface), and phase as well, that means information about distance of radar and exposured point on the Earth. If we do complex multiplication of the first scene with another one (pixel by pixel), we get the interferogram.

2-PASS DIFFERENTIAL INTERFEROMETRY

2-pass differential interferometry is based on an interferometric image pair and a digital elevation model (DEM). The basic idea of 2-pass differential interferometry is that a reference interferogram (interferogram with phase corresponding to surface topography) is simulated based on the DEM. In order to do this the DEM is first transformed from its original coordinate system to the reference SAR image coordinates. This is done in two steps [4]. In a first step the geometric transformation is done based on the available information on the geometry of the DEM and the SAR image geometry used. In the same step the SAR image intensity is simulated based on the simulated local pixel resolution and incidence angle. Inaccurate DEM coordinates, orbit data, and small errors in the calculation of the geometric transformations may result in small offsets between the simulated and the real SAR image geometry. In the second step the offsets between the simulated and real SAR image intensities are estimated and used to accurately register the transformed

DEM to the SAR image geometry. Based on the reference SAR geometry, the interferometric baseline model, and the transformed height map, the unwrapped interferometric phase corresponding exclusively to topography is calculated. In the following this phase will also be called topographic phase.

This method is used to remove the topographically induced phase from the interferogram containing topography, deformation and atmosphere. The temporal baseline should be long enough to allow the deformations to occur, but the deformations cannot be too large.

When used for deformation mapping, the perpendicular baseline should be as short as possible (Table 1) in order to reduce the topographic signal in the interferogram as much as possible.

An important feature of this method is that all measurements are relative. Theoretically, the phase of the differential interferogram should be zero in the areas of no deformation, but there are systematic errors influencing the measurements and therefore the deformations can be determined only relatively with respect to the vicinity [3].

For topographic or deformation monitoring, data selection is often performed with the purpose to eliminate rain and snow. If there is no storm in the mapped area, the atmospheric influence usually has a long-wave characteristic, i.e. it changes slowly in the area [5].

Interferometric processing was performed in the GAMMA software [4]. Data from track 394 for the 2-pass were used. The interferometric pairs are described in Table 1.

Table 1. Interferometric pairs

Interferometric pair	Perpendicular baseline [m]	Sign of a deformation
12501_13503	45	+
14777_15278	8	+
15278_15779	123	+
15779_16280	64	+
23795_23294	4	-
28304_29306	41	+

Table 2. Acquisition dates

Scene	Date
12501	1997-09-10
13503	1997-11-19
14777	1998-02-16
15278	1998-03-23
15779	1998-04-27
16280	1998-06-01
23294	1999-10-04
23795	1999-11-08
28304	2000-09-18
29306	2000-11-27

The differential interferogram for the 2-pass method is filtered and then unwrapped. Due to filtering we achieved much better coherence. Unwrapped phase of that differential interferogram can also be used for a terrain-deformation detection more profitably.

ANALYZES

In Fig 1 we can see landslides in the area of the Slatinice above-level dump. We can evaluate this as 2.7cm for pair 12501_13503 and as 1.6 cm for pair 14777_15278, by means of [2, 6]. Coherence values for pair 12501_13503 are: less than 0.6 8%, 0.6-0.7 4%, 0.7-0.8 11%, 0.8-0.9 43%, more than 0.9 34%. Maximum is 0.964 and minimum is 0.100.

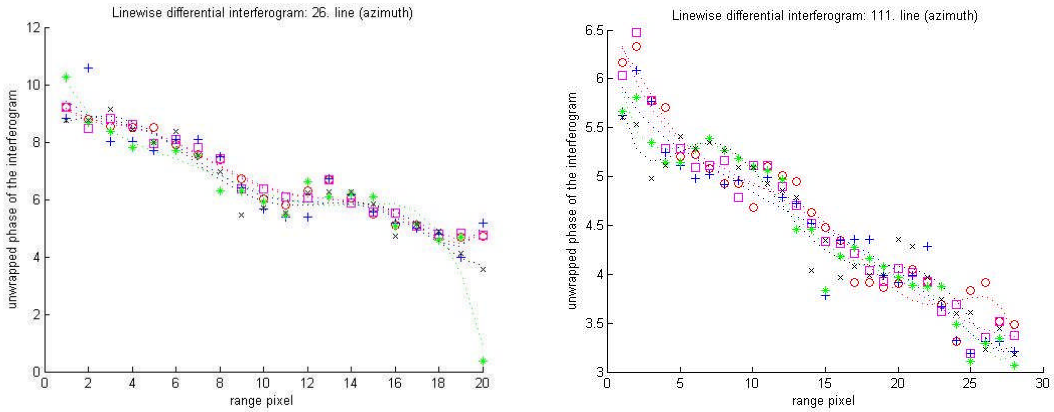

Fig. 1. Differential interferogram where vertical axis is the unwrapped phase of the differential interferogram (in radians). Landslides for interferometric pairs a) 12501_13503, b) 14777_15278.

On the left side of Fig 2a, unwrapped phase of the interferogram is continuous between 3.7 and 5.4 for lines 0-55. Thus the subsidence is 0.8cm. Coherence for these lines 0-55 is higher than 0.95. In place of the highest subsidence (line 15), coherence is 0.99. In the middle of Fig 2b, we confirmed a terrain deformation between range pixels 6 and 23. The unwrapped phase is continuous between 4.8 and 5.7. The subsidence is 0.4cm. Coherence values are between 0.96 and 0.99 for range pixels 6-23. In place of the highest subsidence (pixel 14), coherence is 0.98. Coherence values for pair 14777_15278 are: less than 0.8 0%, 0.8-0.9 1%, more than 0.9 98%. Maximum is 0.996 and minimum is 0.669.

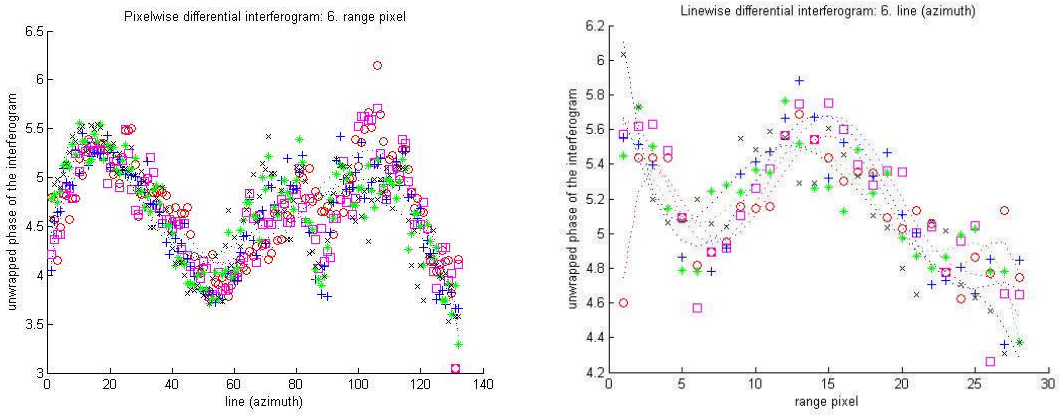

Fig. 2. Differential interferogram where vertical axis is the unwrapped phase of the differential interferogram (in radians). Subsidence for interferometric pair 14777_15278. a) pixelwise interferogram, b) linewise interferogram.

On the left side of the pixelwise differential interferogram in Fig 3a, we can see a terrain deformation. It is a subsidence because of the positive sign of the terrain deformation (Table 1). The values for unwrapped phase of the interferogram are between -9.5 and -11 for lines 0-22. The subsidence for this pair is 0.7 cm. Coherence in the highest subsidence (line 10) is 0.9. That coherence for lines 0-22 is between 0.82 and 0.96. In the linewise differential interferogram (Fig 3b), we evidenced a subsidence as well. The unwrapped phase of the interferogram is between -11.3 and -12.8 for range pixels 13-32. This subsidence is as 0.7cm as in the opposite direction. In place of the highest subsidence (pixel 22), coherence is 0.95. Coherence

values are between 0.8 and 0.96 for range pixels 13-32. Coherence values for pair 15278_15779 are: less than 0.5 0%, 0.5-0.6 1%, 0.6-0.7 2%, 0.7-0.8 8%, 0.8-0.9 33%, more than 0.9 56%. Maximum is 0.975 and minimum is 0.283.

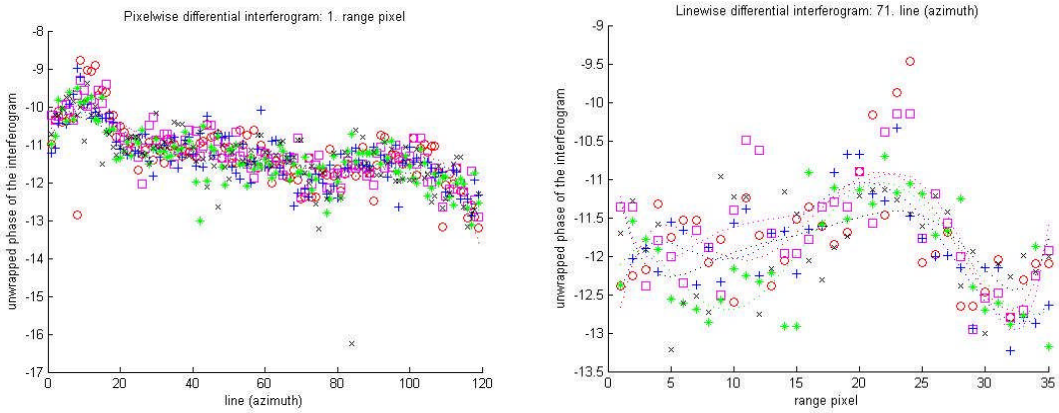

Fig. 3. Differential interferogram where vertical axis is the unwrapped phase of the differential interferogram (in radians). Subsidence for interferometric pair 15278_15779. a) pixelwise interferogram, b) linewise interferogram.

On the left side of Fig 4a, unwrapped phase of the interferogram is continuous between 3.7 and 4.7 for lines 2-55 and on the rigt side of this figure that phase is between 4.0 and 5.7 for lines 92-130. The subsidence on the left side is 0.5cm, and on the right side 0.8cm. Coherence for lines 2-55 is between 0.75 and 0.98. Coherence for lines 92-130 is between 0.75 and 0.97. In places of the highest subsidence (line 27, and 106), coherence is 0.98, and 0.95. Coherence values for pair 15779_16280 are: less than 0.4 2%, 0.4-0.5 4%, 0.5-0.6 4%, 0.6-0.7 4%, 0.7-0.8 10%, 0.8-0.9 30%, more than 0.9 46%. Maximum is 0.988 and minimum is 0.057. In Fig 4b, we confirmed a terrain deformation between range pixels 5 and 15. The unwrapped phase is continuous between -0.8 and -2.5. Thus the subsidence is 0.8cm. Coherence values are between 0.8 and 0.9 for range pixels 5-15. In place of the highest subsidence (pixel 9), coherence is 0.9. Coherence values for pair 28304_29306 are: less than 0.3 5%, 0.3-0.4 3%, 0.4-0.5 4%, 0.5-0.6 6%, 0.6-0.7 13%, 0.7-0.8 20%, 0.8-0.9 32%, more than 0.9 17%. Maximum is 0.965 and minimum is 0.012.

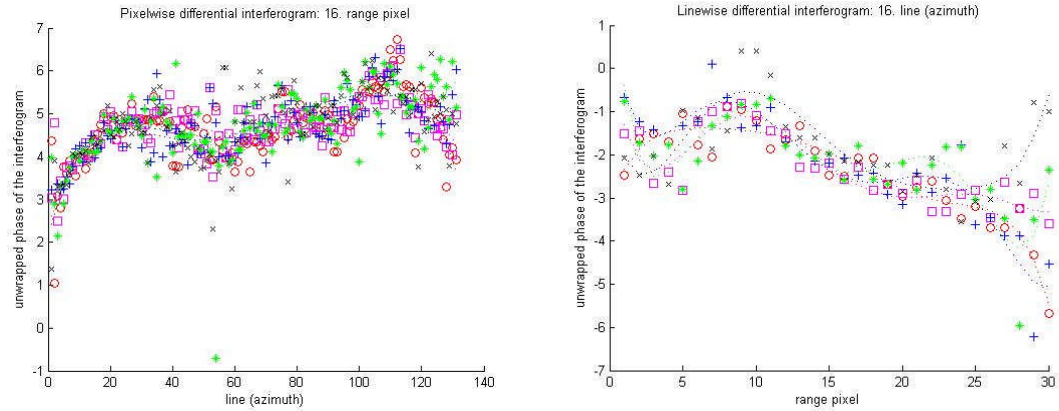

Fig. 4. Differential interferogram where vertical axis is the unwrapped phase of the differential interferogram (in radians). Subsidence for interferometric pairs a) 15779_16280, b) 28304_29306.

On the right side of the pixelwise differential interferogram in Fig 5a, we can see a terrain deformation. It is a subsidence because of the negative sign of the terrain deformation (Table 1). The values for unwrapped phase of the interferogram are between -3 and -4.4 for lines 60-95. The subsidence is 0.7 cm. Coherence in the highest subsidence (line 75) is 0.98. That coherence for lines 60-95 is between 0.96 and 0.99. In the linewise differential interferogram (Fig 5b), we evidenced a subsidence as well. The unwrapped phase of the

interferogram is between -3.3 and -4.1 for range pixels 0-17. This subsidence is 0.4cm. In place of the highest subsidence (pixel 8), coherence is 0.98. Coherence values are between 0.94 and 0.99 for range pixels 0-17. Coherence values for pair 23795_23294 are: less than 0.6 3%, 0.6-0.7 2%, 0.7-0.8 3%, 0.8-0.9 8%, more than 0.9 85%. Maximum is 0.999 and minimum is 0.159.

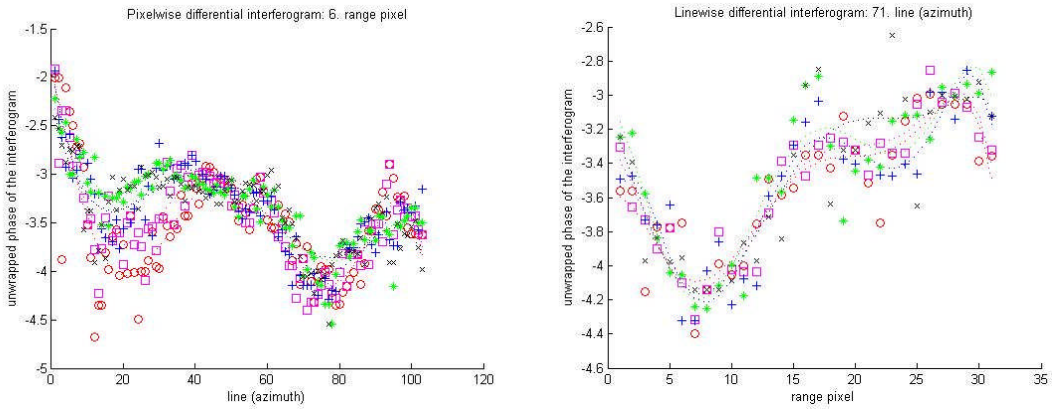

Fig. 5. Differential interferogram where vertical axis is the unwrapped phase of the differential interferogram (in radians). Subsidence for interferometric pair 23795_23294. a) pixelwise interferogram, b) linewise interferogram.

CONCLUSIONS

From our analyzes in previous section, we can do some conclusions. Average subsidence in the area of Slatinice above-level dump is approximately 0.7cm per month. Maximal subsidence we evidenced was 0.8cm for pairs 14777_15278 (pixelwise), 15779_16280 (pixelwise), and 28304_29306 (linewise). These terrain deformations were confirmed by excellent coherence values (0.99, 0.95, and 0.9).

For decision on potential terrain deformation, the suspect areas of subsidence must be sufficiently coherent. For incoherent areas there occurs decorrelation and thus loss of data. We can confuse clearly visible "deformations" in differential interferograms and areas used in agriculture. There are no subsidence and landslides there but only small changes in terrain height in consequence of agricultural cultivation. Terrain could be a little covered with ice as well.

For subsidence confirmation, we demand as continuous phase as possible with a sufficient number of neighboring pixels and lines. We expect coherence values higher than 0.5. After filtering , we obtained much better coherence values. Maximal evaluated coherence was 0.999 for pair 23795_23294. Best coherences values more than 0.9, we obtained for pairs 14777_15278 and 23795_23294. Due to phase unwrapping in the end, we are able to quantify landslides higher than 2.8cm, because that phase is not more between –pi and pi and then there is no phase ambiguity. The perpendicular baseline should be as short as possible, to 50m ideally. However, that baseline for pair 15278_15779 is 123m and nevertheless, a good interference occurred. The time baseline should be as short as possible as well. That is approximately 1 month long or 2 months long exceptionally, for our purposes. When used longer time baselines or longer perpendicular baselines for scenes from stack 394, the decorrelation always occurred.

Terrain deformations (subsidence and landslides) in the area of the Slatinice above-level dump since 1997 until 2000 were evidenced. Further we concentrated on the Jirkov-Most route and railway that slides and is also monitoring and leveled very precisely. Especially its part called the Ervenice corridor. We cannot evidence that area of the Ervenice corridor is stable because of larger variance of the unwrapped-phase values. The results are very decorrelated. In this area, we verified no terrain deformation.

ACKNOWLEDGEMENTS

This article was supported by grant with No. 106/08/0403 GA ČR and by grant Interferometric Determination of Subsidence Caused by Undermining by Permanent Scatterers and Phase Unwrapping Correction within Interferometric Blocs with No. 205/08/0452 GAČR. Data were obtained from ESA within the framework of project Interferometry Used for Landslide and Land Subsidence Detection in the Undermined Area and in the Area with Abandoned Open Brown Coal Mines.

REFERENCES

[1] Bořík, M.: Určení terénních deformací v oblasti Ervěnického koridoru pomocí třísnímkové diferenční interferometrie. Geodetický a kartografický obzor 8/2010, 56/98, 2010, pp. 157-161.

[2] Bořík, M.: Stanovení terénních deformací třísnímkovou diferenční interferometrií. Stavební obzor 5/2009, 2009, pp.150-153.

[3] Bořík, M.- Čapková, I.- Halounová, L.- Kianička, J.: Qualitative distinction between terrain deformations and processing errors, and quantitative description of deformations for the 3-pass interferometry, New Developments and Challenges in Remote Sensing, Millpress, Rotterdam, 2007, pp. 113-121. ISBN 978-90-5966-053-3.

[4] GAMMA Software - http://www.gamma-rs.ch/no_cache/software.html

[5] Hanssen, R.F.: Radar Interferometry: Data Interpretation and Error Analysis. Dordrecht, Kluwer Academic Publishers, 2001.

[6] Kampes, B.: Delft Object-Orientated Radar Interferometric Software: Users Manual and Technical Documentation. Delft, Delft University of Technology, 1999.